Efficient Solutions for Discreteness, Drift and Disturbance (3D) in Electronic Olfaction

Lei Zhang, *Member, IEEE* and David Zhang, *Fellow, IEEE*

Abstract—In this paper, we aim at presenting the new challenges of electronic noses and proposing effective methods for handling the new challenging scientific issues to be solved, such as signal discreteness (reproducibility), systematical drift and non-target disturbances. We first review the progress of E-noses in applications, systems, and algorithms during the past two decades. Recall a number of significant achievements and motivated by the current issues that hinder large-scale application pace of E-nose technology, we propose to address three key issues: discreteness, drift and disturbance (simplified as 3D issues), which are sensor induced and sensor specific. For each issue, a highly effective and efficient method is proposed. Specifically, for *discreteness* issue, a global affine transformation (GAT) method is introduced for E-nose instruments batch calibration; for *drift* issue, an unsupervised feature adaptation (UFA) model is proposed to achieve effective drift adaptation; additionally, for *disturbance* issue, we proposed a simple targets-to-targets self-representation classifier (T^3SRC) method for fast non-targets detection, without knowing any prior knowledge of thousands of non-target disturbances in real world. For each method, a closed form solution can be analytically determined and the simplicity is guaranteed. Experiments demonstrate the effectiveness and efficiency of the proposed methods for addressing the proposed 3D issues in real applications of electronic noses.

Index Terms—Electronic nose, discreteness, drift, disturbance, sensor

I. INTRODUCTION

Electronic olfactory system constructed with a model nose was proposed for the first time to mimic the biological olfactory mechanism as early as in 1982 [1], which presented two key assumptions of mammalian olfactory system: (1) there is no requirement for odour-specific transducers; (2) odor signals from the transducers can be learnt. One key characteristic of model nose is that the odorant detectors (i.e. the primary neurons) respond to a wide range of chemicals. In 1994, Gardner *et al.* [2] showed a new definition for artificial olfactory system: "An electronic nose is an instrument, which comprises an array of chemical sensors with partial specificity and an appropriate pattern recognition system, capable of recognizing simple or complex odours". In other words,

electronic nose (abbreviated as E-nose) can be recognized to be an intelligent sensor array system for mimicking biological olfactory functions. An excellent review of E-noses can be referred as [3]. A general electronic nose system in research route is presented in Fig. 1, which consists of data acquisition and pattern recognition. The sensor array chamber with controller is recognized to be an E-nose device.

A. Development in Application Level

E-nose has been applied in many areas, such as food analysis [4-13], medical diagnosis [13-17], environmental monitoring [18-23], and quality identification [7,8,24,25]. For *food analysis*, Brudzewski *et al.* [4] propose to recognize four different types of milk, Lorenzen *et al.* [5] tends to differentiate four types of cream butter, Bhattacharyya *et al.* [6] proposed to classify different types of black tea, Chen *et al.* [7], Dutta *et al.* [8], Hui *et al.* [9] and Varnamkhasti *et al.* [10] propose to predict tea quality, apple storage time and the aging of beer. The reviews of the existing work in food control and analysis by using E-noses are referred as [11-13]. For *medical diagnosis*, inspired by [14] that human breath contains some biomarkers that contribute to disease diagnosis, Yan and Zhang [15] proposed a breath analysis system to differentiate healthy people and diabetics, Di Natale *et al.* [16] proposed a lung cancer identification system with a quartz microbalance (QMB) sensor array, Pavlou *et al.* [17] designed a 14-conducting polymer sensor array for diagnosis of urinary tract infections. For *environmental monitoring*, Getino *et al.* [18] and Wolfrum *et al.* [19] proposed to detect the volatile organic compounds (VOCs) in air, Zhang *et al.* [20, 21] proposed a portable E-nose system for concentration estimation using neural networks, targeting at real-time indoor air quality monitoring, Dentoni *et al.* [22], Baby *et al.* [23] and Fort *et al.* [24] proposed tin-oxide sensors based systems for monitoring air contaminants, including single odour and mixtures of different odours. For *quality identification*, Chen *et al.* [7] and Dutta *et al.* [8] proposed to discriminate and predict tea quality, Gardner *et al.* [25] proposed to monitor the quality of potable water, and Cano *et al.* [26] proposed to discriminate counterfeits of perfumes.

Other applications are referred as tobacco recognition [27], coffee recognition [28], beverage recognition [29], and explosives detection [30], etc. To this end, we refer to interested readers as [31] for extensive applications of E-noses.

B. Development in System Level

After observing a number of E-nose applications, we then present different types of E-noses systems, like conventional

● L. Zhang is with the College of Communication Engineering, Chongqing University, Chongqing 400044, China. (e-mail: leizhang@cqu.edu.cn)
● D. Zhang is with the Department of Computing, The Hong Kong Polytechnic University, Hung Hom, Hong Kong. (e-mail: csdzhang@comp.polyu.edu.hk)

1-Pump with flow-meter;
2-Sensor chamber;
3-Personal computer;
4-Valve;
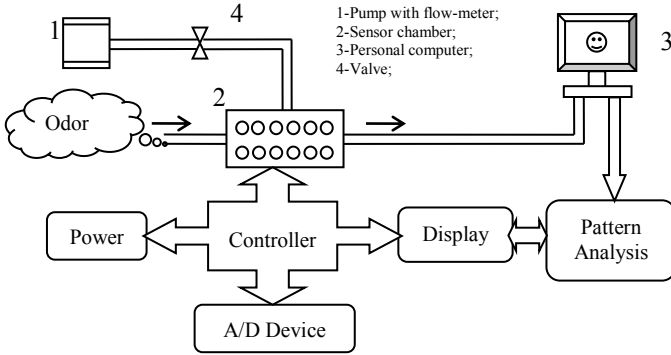
Fig. 1. A general electronic nose system with multiple units

E-noses [32-35], differential E-noses [27, 28, 30], temperature modulated E-noses [36-41], active E-noses [42-44] and LabView E-noses [45, 46]. *First*, the conventional E-noses are constructed with a sensor array worked at constant temperature voltage. Zhang *et al.* [32, 33] proposed a 6-metal oxide semiconductor gas sensor system, Hong *et al.* [34] proposed a 6-thick film oxide sensor system, and Rodriguez-Lujan *et al.* [35] proposed a 16-screen printed MOX gas sensing system. *Second*, the differential E-nose proposed by Brudzewski *et al.* [27, 28, 30] is with two sensor arrays: one is for gas sensing and the other one is for baseline measurement. *Third*, the temperature modulated E-noses proposed by Lee and Reedy [36], Llobet *et al.* [37], Martinelli *et al.* [38], Hossein-Babaei and Amini [39, 40], and Yin *et al.* [41] are with an idea that the heating voltage of each sensor is dynamic rather than constant. The adaptive change (ramp, sine wave, rectangular wave, etc.) of heating voltage is termed as temperature modulation. The rationality behind is that one sensor with multiple heating voltages would produce multiple patterns, such that temperature modulation can effectively lower the cost of sensor array [41]. *Fourth*, the active E-noses proposed by R. Gosangi *et al.* [42, 43] and Herrero-Carrón *et al.* [44] are evolution of temperature modulation systems. The "active" concept shows an adaptive optimization of operating temperatures, because not all heating voltages contribute positively to classification. *Lastly*, Imahashi and Hayashi [45] developed a computer controlled odor separating system based on LabVIEW, which consists of adsorbing and separating cells. It separates the detected odorants in terms of the properties of installed adsorbents. Jha and Hayashi [46] also developed a LabVIEW based odor filtering system. The advantage of LabVIEW based E-noses are low-cost, high efficiency and heuristic for lab use.

C. Paper Organization

After an overview, the progress of E-nose is significant. Our purpose is to study soft computing algorithms in E-noses. Therefore, in this paper, we focus on the new challenges after a thought of technical issues that prevents the industrialization paces of E-noses. Further, we propose efficient solutions in facing with the challenges. A general diagram of the progress and challenges is illustrated in Fig. 2. The parts in bright blue color and orange color denote the achieved aspects and new challenges in its current stage.

The remainder of this paper is as follows. Section II illustrates the key achievements of state-of-the-art algorithms. Section III presents the 3D issues with the proposed methods, solutions and experiments. Finally, Section IV concludes this paper and conceives the future work.

II. RELATED WORK IN ALGORITHM LEVEL

A. Feature Extraction and De-noising Algorithms

Feature extraction is the first step of a recognition system. Without exception, multi-dimensional feature extraction is also the key part of E-nose system. Generally, hand-crafted feature extraction includes normalization, feature selection and feature enhancement [47]. *Normalization* is used to remove the scaling effect caused by odorant concentration, such that the interrelation among patterns can be better shown. Suppose the original feature matrix $\mathbf{X} = [\mathbf{x}_1, \cdots, \mathbf{x}_n] \in \mathfrak{R}^{d \times n}$, then the normalization is formulated as follows

$$x_{ij} = x_{ij}/\max(\mathbf{x}_i), i = 1, \cdots, d; j = 1, \cdots, n \quad (1)$$

where d and n denotes the feature dimension and the number of samples, respectively. More normalization techniques such as baseline subtraction, centralization, scaling, etc. can be found in [47]. *Feature selection* aims at identifying the most informative and discriminative subset that leads to the best classification performance [51]. Principal component analysis (PCA) and linear discriminant analysis (LDA) are used for extracting the most informative and discriminative features, respectively. Suppose $\mathbf{W} \in \mathfrak{R}^{d \times k}$ to be the linear transformation (basis), the extracted features $\hat{\mathbf{X}}$ is as follows

$$\hat{\mathbf{X}} = \mathbf{W}^{\mathrm{T}}\mathbf{X} \quad (2)$$

where k denotes the number of selected components (eigenvectors). Further, Peng *et al.* [48] proposed a KECA method by considering the components *w.r.t.* maximum entropy, rather than maximum eigenvalue. Martinelli *et al.* [49] proposed a phase space based feature extraction with temporal evolution of sensor response. Leone *et al.* [50] proposed a representation method, which solves a dictionary algorithm by minimizing reconstruction error. *Feature enhancement* targets at the best features in another domain (e.g. frequency domain). Ehret *et al.* [52] proposed a Fourier transform method without information loss, and Kaur *et al.* [53] proposed a dynamic social impact theory and moving window time slicing method.

De-noising algorithms pursue noise removal (i.e. de-noising) on data mixed with some unknown noise. First, in pre-processing, smooth filter (window moving average) in real-time sensing was used [54]. Suppose the response sequence to be $\{S(i), i = 1, \cdots, Q\}$, the filtered response is

$$\hat{S}(j) = \frac{\sum_{i=j}^{j+q-1} S(i) - \max\{S(j), \cdots, S(j+q-1)\} - \min\{S(j), \cdots, S(j+q-1)\}}{q-2} \quad (3)$$

where Q and q represent the length of signal and smooth filter, $j = 1, \cdots, Q - q + 1$. Moreover, Kalman filter was used [55]. Second, in feature extraction, Jha and Yadava [56] proposed singular value decomposition (SVD) based denoising. The noise removal is done by truncating the components *w.r.t.* a few largest singular values and reconstructing the noiseless data as

$$\hat{\mathbf{X}} = \sum_{i=1}^{k} \hat{\sigma}_i \mathbf{u}_i \mathbf{v}_i^{\mathrm{T}} \quad (4)$$

where $\hat{\sigma}_i$ represents the truncated singular value, $\mathbf{u}_i$ and $\mathbf{v}_i$ represent the singular vectors *w.r.t.* $\hat{\sigma}_i$, k denotes the rank of
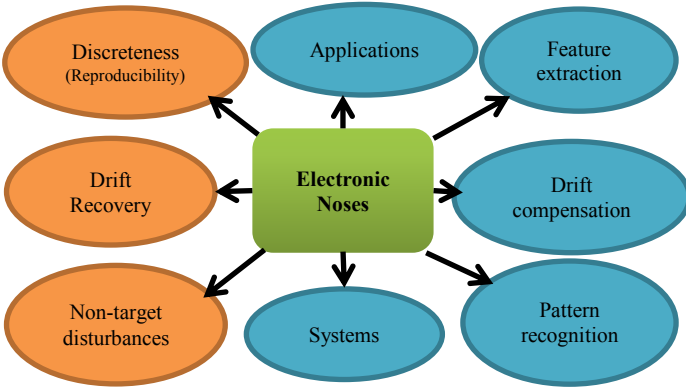
Fig. 2. Developments (*blue*) and Challenges (*orange*) of E-Noses

noiseless data (i.e. $\hat{\sigma}_i = 0$ for $i > k$). The principle of SVD can be referred as [57]. Furthermore, following component analysis based methods, Di Natale *et al.* [58], Kermit and Tomic [59] proposed higher order statistical method, i.e. independence component analysis (ICA) based denoising, which shows better representation for non-Gaussian data than PCA. The ICs that are highly correlated with disturbance will be recognized as noise. Suppose that $\mathbf{X} = [\mathbf{x}_1, \cdots, \mathbf{x}_n]^{\mathrm{T}} \in \Re^{n \times d}$ is mixed by source signal $\mathbf{S} = [\mathbf{s}_1, \cdots, \mathbf{s}_m]^{\mathrm{T}} \in \Re^{m \times d}$ through a linearly mixed system $\mathbf{A} \in \Re^{n \times m}$, then there is

$$\mathbf{X} = \mathbf{AS} \tag{5}$$

ICA aims at solving a linear transform or un-mixing system $\mathbf{W} \in \Re^{m \times n}$, and the estimated source signal $\hat{\mathbf{X}}$ is formulated as

$$\hat{\mathbf{X}} = \mathbf{WX} = \mathbf{WAS} \approx \mathbf{S} \tag{6}$$

where $\hat{\mathbf{X}} \approx \hat{\mathbf{S}}$ and $\mathbf{W} \approx \hat{\mathbf{A}}^{-1}$. By solving $\mathbf{W}$, the unmixed source signal can be recovered. Tian *et al.* [60] also proposed a hybrid PCA plus ICA de-nosing. We refer to as [47, 61, 62] for more knowledge about signal processing in E-nose.

B. Pattern Recognition Algorithms

Pattern recognition methods are powerful tools to endow E-nose with "intelligence". Therefore, conventional pattern recognition algorithms such as nearest neighbors [63, 64], neural networks [65, 66], support vector machines (SVMs) [63, 68, 69] and decision tree [70] have been proposed for E-nose applications. Some improved SVMs are also proposed. For example, Wang *et al.* [71] proposed a relevance vector machine (RVM) with fewer kernel functions, Zhang *et al.* [72] proposed a hybrid support vector machine (HSVM) with fisher linear discriminant analysis, and Vergara *et al.* [73] proposed an inhibitory support vector machine (ISVM), inspired by the inhibition process in animal neural system. Recently, *committee classifiers* (ensemble models) are used in E-nose for classification. For example, Shi *et al.* [74] proposed a committee machine (GIEM) combined with five algorithms (experts) in decision level, Szczurek *et al.* [75] proposed a multiple classifiers system (MCS) of four sensor-specific base classifiers, and Dang *et al.* [76] proposed an improved support vector machine ensemble (ISVMEN) method with base classifier weighting. *Fuzzy algorithms* have also been proposed in E-nose. For example, Tudu *et al.* [77] proposed an incremental learning fuzzy approach for black tea classification,

and Jha *et al.* [78] proposed an adaptive neuro-fuzzy inference system (ANFIS). Recently, *semi-supervised learning* has been used in E-nose for dealing with more challenging problem (i.e. insufficient labeled data). Specifically, De Vito *et al.* [79] proposed a semi-supervised learning technique (COREG) based on cluster assumption, and Hong *et al.* [80] also proposed to use cluster based semi-supervised approach for E-nose data. From the analysis above, E-nose has observed a progress in pattern recognition algorithms. We refer to readers as [81] for an insight of pattern analysis methods in machine olfaction.

C. Drift Compensation Algorithms

Though much endeavor has been made on algorithms, sensor drift caused by unknown dynamic processes (aging, poisoning, etc.) is seriously deteriorating classification [82]. From the viewpoint of machine learning, the drifted data cannot well fit the training data due to their differences in probability distribution, and classifier re-training/recalibration with new samples is required. In the past 10 years, a progress is observed in drift compensation. Zuppa *et al.* [83] proposed a multiple self-organizing maps method, by adapting each map to the changes of input probability distribution. Ding *et al.* [84] proposed a hybrid method of PCA and wavelet for detecting drift online, and then compensate it using an adaptive dynamic drift compensation algorithm (ADDC). The drift model of each sensor can be dynamically updated online, which assumes that there exists some linear/nonlinear relation between drift and time. Artursson *et al.* [85] proposed a component correction based principal component analysis (CCPCA) method, by finding the drift direction and correct the data. The model of component correction is shown as follows

$$\hat{\mathbf{X}} = \mathbf{X} - (\mathbf{Xp})\mathbf{p}^{\mathrm{T}} \tag{7}$$

where $\mathbf{p}$ is the loading vector (drift direction) calculated by PCA on the reference gas data with serious drift, $\mathbf{X}$ is the measurement data and $\hat{\mathbf{X}}$ is the drift component corrected data. Ziyatdinov *et al.* [86] proposed a common principal component analysis (CPCA) method, which explicitly computes the drift direction for all classes. Padilla *et al.* [87] proposed a linear orthogonal signal correction (OSC) by removing the components (e.g. drift components) orthogonal to the data. The correction model is shown as

$$\hat{\mathbf{X}} = \mathbf{X} - \sum_{i=1}^{n} \mathbf{t}_i \mathbf{p}_i^{\mathrm{T}} \tag{8}$$

where n denotes the number of OSC factors, $\mathbf{p}_i$ is the loading vector and $\mathbf{t}_i$ is the score vector.

Additionally, Di Carlo *et al.* [88] proposed an additive factor correction method, in which the correction matrix is optimized by using evolutionary algorithm (EA), described as

$$\hat{\mathbf{X}} = \mathbf{X} + \mathbf{XM} \tag{9}$$

where $\mathbf{M}$ is the optimized correction factor by using EA.

These methods suppose that drift can be corrected additively, but capability restricted due to its nonlinear dynamic behavior [89]. To this end, Vergara *et al.* [90] proposed a classifier ensemble method for enhancing the classifier generalization to drift and also provided a long-term drift dataset for validation. Liu *et al.* [91] also proposed a fitting based dynamic classifier ensemble. Martinelli *et al.* [92] proposed an AIS based adaptive classification method. Recently, transfer learning based models

have been proposed by Liu *et al.* [93] and Zhang *et al.* [94] for drift adaptation and the classification accuracy on drifted data has been much improved. The DAELM transfer learning model proposed in [94] for drift adaptation is formulated as follows

$$\min_{\boldsymbol{\beta}_S, \boldsymbol{\xi}_S^i, \boldsymbol{\xi}_T^i} \frac{1}{2}\|\boldsymbol{\beta}_S\|^2 + C_S \frac{1}{2}\sum_{i=1}^{N_S}\left\|\boldsymbol{\xi}_S^i\right\|^2 + C_T \frac{1}{2}\sum_{j=1}^{N_T}\left\|\boldsymbol{\xi}_T^j\right\|^2 \quad (10)$$

$$\text{s.t.}\begin{cases} \mathbf{H}_S^i\boldsymbol{\beta}_S = \mathbf{t}_S^i - \boldsymbol{\xi}_S^i, i = 1, \dots, N_S \\ \mathbf{H}_T^j\boldsymbol{\beta}_S = \mathbf{t}_T^j - \boldsymbol{\xi}_T^j, j = 1, \dots, N_T \end{cases} \quad (11)$$

where $\boldsymbol{\beta}_S$ is the learned classifier with drift adaptation, $\mathbf{H}_S$ and $\mathbf{H}_T$ denote the hand-crafted data matrix for clean and drifted sensor data, $\mathbf{t}_S$ and $\mathbf{t}_T$ denote the label matrix, $\boldsymbol{\xi}_S$ and $\boldsymbol{\xi}_T$ denote the prediction error on source and target data, respectively.

From the discussions in the previous sections, E-nose has witnessed significant progress in *applications*, *systems*, *feature extraction*, *pattern analysis* and *drift compensation* aspects. However, for industrialization, commercialized E-noses still face with several novel challenges, such as *discreteness* (reproducibility), *drift* recovery and non-target *disturbance* counteraction. These challenges are closely related with the fate of E-nose technology in large-scale industrialization. Therefore, in this paper, we aim at proposing these challenges in terms of the current E-noses, and also proposing the highly efficient solutions for dealing with the key problems.

III. PROPOSED 3D ISSUES, METHODS AND SOLUTIONS

A. Notations

In this paper, $\mathbf{X}_S \in \mathfrak{R}^{d \times N_S}$ and $\mathbf{X}_T \in \mathfrak{R}^{d \times N_T}$ represent the source and target domain data, d is the data dimension, and N_S and N_T represent the size of source and target data. a_k and b_k represent the calibration transfer coefficient for sensor k. $\mathbf{x}_i$ denotes the i-th obervation, $\mathbf{P}_S \in \mathfrak{R}^{d \times r}$ and $\mathbf{P}_T \in \mathfrak{R}^{d \times r}$ denote the subspace projection (basis) of source and target domain, and r denote the lower dimension. $\mathbf{W}$ represents the subspace alignment. $\boldsymbol{\alpha}$ denotes the representation coefficient matrix, $\|\cdot\|_F$ denotes the Frobenius norm, $\|\cdot\|_2$ denotes l_2-norm and $(\cdot)^{-1}$ denotes the inverse operator.

B. 3D Challenge I: Discreteness

Reproducibility represents the signal discrepancy of multiple E-nose systems with identical sensor array. It is known that in the sensor manufacturing process the inherent variability may cause slight difference in the reactivity of the tin oxide substrate, such that the response of two identical sensors under the same condition is different [95]. This discrepancy between two identical sensors can be termed as sensor discreteness [96], which results in the worse reproducibility problem of E-noses. From the viewpoint of E-nose system, sensor discreteness reflects the output differences (signal shift) among completely the same E-nose systems. Specifically, the discreteness can be described as two facets [96]. (1) baseline difference: the sensitive resistance R_o of two identical sensors in clear air under the same ambient temperature and relative humidity is different, which results in that the response (output voltage) of the identical sensors is also different; (2) sensitivity difference: two identical sensors that exposed to some odorant have different sensitivity R_s/R_o, where R_s is the sensitive resistance in odorant and Ro in clean air, such that the responses of two sensors are
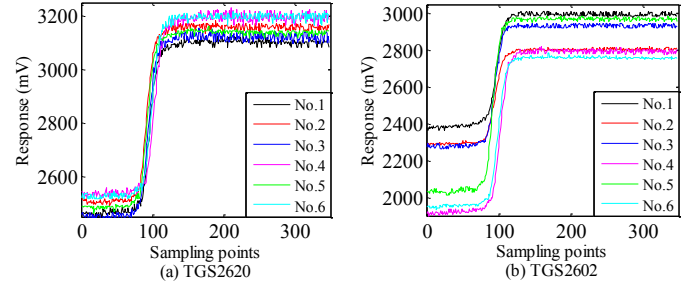
Fig. 3. Characteristic of sensor discreteness. Six sensors are repeated.

also different. More visually, the discreteness can be observed in Fig.3, where Fig. 3(a) denotes the response of the same 6 TGS2620 sensors under the same condititon, and Fig. 3(b) shows the response of the same 6 TGS2602 sensors.

From the analysis above, the discreteness greatly deteriorates the predictive performance of multiple E-nose systems, which particularly prohibits the large-scale production of E-noses. Therefore, it is urgent and challenging to enhance the reproducibility for accelerating the development of E-nose technology. In the present literatures, most of the E-nose research focus on one single system but neglects the systematical discrepancy among multiple systems. Therefore, the pattern recognition algorithms established on single system cannot be used in multiple systems if the discrepancy is not well handled. For this purpose, Tomic *et al.* [97] proposed a univariate direct standardization (UDS) and a partial least square based PLS2 method for handling the instrument shift. However, the two methods tend to reduce the shift by matrix based standardization, but neglect the property of sensor-specific discreteness. Zhang *et al.* [98] also proposed matrix standardization by using nonlinear artificial neural network for compensating the nonlinear instrument shift.

In our research, as discussed in [99], we found that the discreteness is sensor-specific and approximately linear in some affine space. Therefore, to address this challenge we propose a very simple and effective global affine linear transformation (GAT) model for discreteness reduction and reproducibility enhancement, which is formulated as follows

$$\mathbf{y}_k = a_k \mathbf{x}_k + b_k, k = 1, \cdots, m \quad (12)$$

where $\mathbf{x}_i$ denotes the i-th sensor response of the *slave* instrument, $\mathbf{y}_i$ denotes the i-th sensor response of the *master* instrument, a_i and b_i represent the sensor-specific calibration parameters. The parameters can be easily solved by using regularized least square based methods.

For computing the calibration coefficients in (12), several global optimal samples should be selected from the training set due to that in large scale calibration transfer, the sample collection needs high labor cost. Therefore, a Euclidean distance based sample selection algorithm (SSA) is presented for searching the most representative samples, which is described as follows.

Step 1: Calculate the Euclidean distance in pair-wise from the master training set, and select the farthest two patterns s_1 and s_2 as the calibration samples, which forms a set $S = \{s_1, s_2\}$.

Step 2: To each sample $\mathbf{x}_i$, the Euclidean distance between $\mathbf{x}_i$
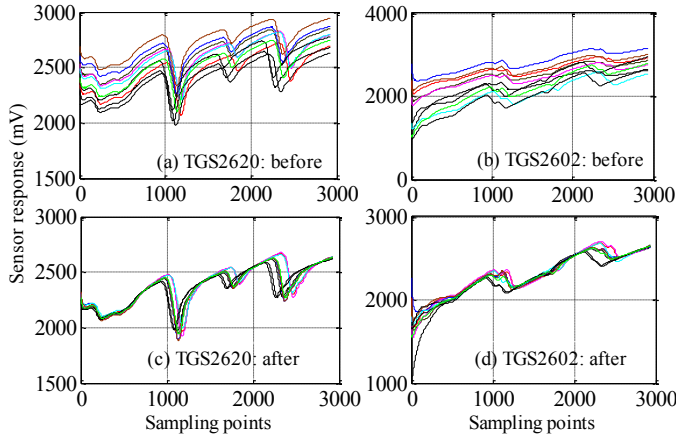
Fig. 4. Sensors discreteness before and after correction of 10 identical E-nose instruments

Fig. 5. Schematic diagram of UFA for drift (subspace) adaptation

and one sample in set S is computed and the nearest distance is denoted as d_i, which then forms a nearest distance vector $\mathbf{d}$.

Step 3: The sample with the farthest distance in $\mathbf{d}$ is selected as the calibration sample s_3, and update the set $S = \{s_1, s_2, s_3\}$.

Step 4: repeat Step 2, Step 3, until calibration set S is done.

In this paper, five samples i.e. $S = \{s_1, s_2, s_3, s_4, s_5\}$ are selected for calibration transfer by using model (12). The coefficients will be used for on-line calibration in real-time use.

The proposed method can be easily implemented for sensor discreteness reduction in large-scale E-nose systems coupling with operable experimental procedures for different odorants [96]. The performance of sensor discreteness calibration of 10 E-nose systems with identical type is shown in Fig. 4, from which we can clearly observe the reproducibility enhancement of E-noses. Specifically, Fig. 4(a) and (c) show the sensor discreteness before and after correction of TGS2620 signal, respectively, and that of the TGS2602 is shown in Fig. 4(b) and (d) by using GAT method. In terms of Fig. 4(a) and (b), we can figure out the difficulties of E-noses in large-scale production due to the very bad reproducibility. Therefore, reproducibility enhancement is one challenge on the road of E-nose industrialization and the proposed affine linear model would be a very efficient solution in large-scale E-nose calibration [96].

C. 3D Challenge II: Drift

Drift is another challenge, due to that the sensor array is the most important part in E-noses which provides source signal of odorants. In the past two decades, drift has been paid more attention with different drift counteraction and compensation techniques. However, drift still plagued researchers and prohibit the long-term and stable usage of E-noses. In principle, drift has been caused by a number of factors, such as aging, ambient temperature, humidity, pressure and poisoning, etc. such that the chemical reaction inside the sensors when exposed to some odorant will be broken. Therefore, it is difficult to establish a drift model once and for all, especially that the sensor with identical type shows different drift effects. In our opinion, drift cannot be explicitly shown but may be implicitly learned through enough prior knowledge. Therefore, in this paper, we propose a very simple but effective *Unsupervised Feature Adaptation* (UFA) based transfer learning idea for enhancing the drift tolerance of E-noses, such that the aging and performance can be extended and optimized. The previous method (DAELM) in [94] is a supervised classifier adaptation method and the information of labels is needed for classifier learning. However, in large-scale drift data, it becomes difficult to label each sample by hand. Therefore, an unsupervised and subspace transfer learning based feature adaptation (UFA) is proposed and discussed in this paper, instead of classifier adaptation. Specifically, the proposed UFA aims at minimizing the distribution discrepancy in principal component (PC) subspace caused by drift. By aligning the PC subspace between the clean E-nose data and the drifted data, the drift can be well compensated. The idea of the proposed UFA is described in Fig. 5, from which the aligned subspace for source and target data is achieved. Visually, the data distribution in principal component space has been shown in Fig. 6, in which Fig. 6 (a) shows the principal component loading vectors of 10 batches and Fig. 6 (b) shows the low-dimensional projection of the data on the principal component space. Note that the 10 batches of E-nose data were provided by Vergara *et al.* [90], which were collected during 3 years and the batch 1 is recognized to be clean data without drift. From Fig. 6, we can clearly observe the distribution discrepancy of the loading vectors and the principal component projection between batch 1 and other batches, due to the drift effect.

● **UFA: Unsupervised Feature Adaptation**

The UFA idea described in Fig. 5 is for adapting the subspace incrementally learned from old data to new drift data observed by an E-nose. In this section, we will discuss a subspace transfer learning model in feature-level (i.e. feature adaptation). It is known to us that the difference between the un-drifted sensory data and the drift data lies in the probability distribution discrepancy. Let each batch of data be a domain, that is, the clean (no drift) data is viewed as source domain $\mathbf{X}_S \in \Re^{d \times N_S}$ and the drift data is viewed as target domain $\mathbf{X}_T \in \Re^{d \times N_T}$. Then, the drift compensation issue can be recognized to be a domain adaptation or transfer learning problem from source domain to target domain. For domain adaptation, in this paper, we make use of the subspace $\mathbf{P}_S \in \Re^{d \times r}$ and $\mathbf{P}_T \in \Re^{d \times r}$ composed of r eigenvectors induced by PCA, of source and target domain, respectively. We suggest project the source and target data into their respective subspace $\mathbf{P}_S$ and $\mathbf{P}_T$, by using $\mathbf{P}_S^T \mathbf{X}_S$ and $\mathbf{P}_T^T \mathbf{X}_T$. For feature subspace adaptation, we propose a simple model by

---

Algorithm 1: UFA

Input: $\mathbf{X}_S$ and $\mathbf{X}_T$;
Output: $\mathbf{W}^*$, $\mathbf{X}_T^{new}$ and $\mathbf{X}_S^{new}$;
Step 1: Solve $\mathbf{P}_S$ by using PCA on $\mathbf{X}_S$;
Step 2: Solve $\mathbf{P}_T$ by using PCA on $\mathbf{X}_T$;
Step 3: Obtain $\mathbf{W}^*$ by solving the model Eq. (14);
Step 4: Calculate $\mathbf{X}_T^{new}$ by using Eq. (15);
Step 5: Compute $\mathbf{X}_S^{new} = \mathbf{P}_S^{\mathrm{T}}\mathbf{X}_S$.

---

aligning $\mathbf{P}_S$ and $\mathbf{P}_T$ with a linear transformation, as follows

$$\min_{\mathbf{W}}\|\mathbf{P}_S - \mathbf{P}_T\mathbf{W}\|_F^2 + \lambda\|\mathbf{W}\|_F^2 \qquad (13)$$

where $\|\cdot\|_F$ denotes the Frobenius norm and $0 \leq \lambda \leq 10$ denotes a positive regularization coefficient. Consider the orthogonal property of r eigenvectors in each domain, the model (13) can be written as

$$\mathbf{W} = (\mathbf{P}_T^{\mathrm{T}}\mathbf{P}_T + \lambda\mathbf{I})^{-1}\mathbf{P}_T^{\mathrm{T}}\mathbf{P}_S = \frac{1}{\lambda+1}\mathbf{P}_T^{\mathrm{T}}\mathbf{P}_S \qquad (14)$$

where $\mathbf{P}_T^{\mathrm{T}}\mathbf{P}_T = \mathbf{I}$. If there is no difference between $\mathbf{X}_S$ and $\mathbf{X}_T$, then $\mathbf{W}^* = \frac{1}{\lambda+1}\mathbf{P}_T^{\mathrm{T}}\mathbf{P}_S = \frac{1}{\lambda+1}\mathbf{I}$, and the $\frac{1}{\lambda+1}$ can be recognized to be the scaling coefficient.

With the optimal $\mathbf{W}^*$, the drift-less target data with the adapted subspace basis vectors can be formulated as follows

$$\mathbf{X}_T^{new} = (\mathbf{P}_T\mathbf{W}^*)^{\mathrm{T}}\mathbf{X}_T = \frac{1}{\lambda+1}\mathbf{P}_S^{\mathrm{T}}\mathbf{P}_T\mathbf{P}_T^{\mathrm{T}}\mathbf{X}_T \qquad (15)$$

As we can see from the UFA method, during subspace transfer process, the labels are not considered. Therefore, UFA can be recognized to be unsupervised feature adaptation. Generally, the UFA algorithm is summarized as Algorithm 1.

● **Experiments**

The long-term (3 years) sensor drift data published in UCI Machine Learning Repository by Vergara *et al.* [90] has been used for verifying the proposed UFA method. The dataset consists of 13,910 observations by an E-nose with 16 gas sensors on 6 kinds of odorants, such as acetone, acetaldehyde, ethanol, ethylene, ammonia and toluene. In feature extraction, 8 features on each sensor are selected which forms a 128-dimensional vector for each observation. This time series dataset is divided into 10 batches in terms of the experimental period. Therefore, the batch 1 is recognized to be drift-less (clean) data, and there is more and more serious drift from batch 2 to batch 10. The number of samples in each batch is shown in Table I. For classification, we train a support vector machine with RBF kernel on the raw data (RAW$_{SVM}$), semi-supervised learning (SSL) with manifold structure preservation, CCPCA and the adapted feature using UFA (UFA$_{SVM}$), respectively. In experiment, we take the batch 1 as source data without drift for classifier learning and test on other batches. For the proposed UFA method, the projected $\mathbf{X}_S^{new}$ of the batch 1 is used for classifier training and the projected $\mathbf{X}_T^{new}$ with drift adaptation via UFA is used for testing. We have compared with RAW$_{SVM}$, CCPCA and SSL methods for confirming the effectiveness of the proposed UFA method.

First, we have plotted the principal component loading vectors and low-dimensional projection after UFA treatment in Fig. 7. By comparing the scatter points shown in Fig. 6, it is clearly observed that the distribution has been aligned and the similarity of the loadings has been enhanced after using the proposed UFA based drift compensation algorithm. Further, for quantifying the distribution difference, we propose to use a metric which is defined as Mean Distribution Discrepancy

(MDD). Specifically, the *MDD* between $\mathbf{\Theta}_1 \in \mathfrak{R}^{N_1 \times r}$ and $\mathbf{\Theta}_2 \in \mathfrak{R}^{N_2 \times r}$ is calculated as follows

$$MDD(\mathbf{\Theta}_1, \mathbf{\Theta}_2) = \left\|\frac{1}{N_1}\sum_{i=1}^{N_1}\mathbf{\theta}_{1(i)} - \frac{1}{N_2}\sum_{j=1}^{N_2}\mathbf{\theta}_{2(j)}\right\|_2 \qquad (16)$$

where $\mathbf{\theta}_{1(i)}$ and $\mathbf{\theta}_{2(j)}$ denote the i-th and j-th row vectors.

The MDD between batch 1 and other batches in the principal component loading vectors is presented in Table I (Loadings_RAW vs. Loadings_UFA), and that of the projection with the loadings is also presented in Table I (Projection_RAW vs. Projection_UFA). From the Table I, the quantitative difference of the raw data and drift-adapted data via UFA is significant. The classification accuracy has been reported in Table II, from which we can observe the much improved performance with 6.3% increment on average. Additionally, for statistical test on the results, we adopt *t-test* and *ANOVA-test* on Table I and II, respectively. The test result shows a statistical significance with a level of 5%.

From the experimental data analysis, the effectiveness of the proposed UFA is demonstrated. The advantages of UFA can be summarized as three points: 1) UFA aims at aligning the subspace distribution of the E-nose data, instead of exploring the drift direction or some deterministic rules that are not robust and generalized in large-scale gas sensors. 2) UFA is an unsupervised machine learning method, such that it can reduce a lot of work in labeling each sample and overcome the flaws of the classifier adaptation based drift compensation methods. 3) UFA is simple in implementation and can be easily achieved with high efficiency. UFA provides a new idea from subspace adaptation in facing with the E-nose drift challenge.

D. 3D Challenge III: Disturbances

In this section, we will present the third challenge, *non-target disturbance*, which has seriously caused a failure of E-nose in real-time applications. For better understanding the "non-target disturbance", we call the odorants that will be measured as target gases. Therefore, the non-target gases other than the several target odorants being detected are uniformly recognized to be the "disturbances". For our E-nose system, six odorants such as formaldehyde, benzene, toluene, carbon monoxide, ammonia, and nitrogen dioxide are the target gases being tested. Specifically, any unknown odorant except the six target gases would be viewed as disturbance, such as alcohol, perfume, smoke smell, fruit smell, etc. because the metal oxide semiconductor gas sensors produce much stronger response to these disturbances that are undesired, as shown in Fig. 8. The experiment in Fig. 8 is as follows. First, the baseline is collected in the first 2 minutes. Second, the disturbance is within the next 5 minutes. Third, the disturbance exhaust continues about 10 minutes. Fourth, repeat the three steps four times. Although the non-target disturbance is serious, research on this specific problem has never been reported in E-nose community except [54], in which the non-target disturbances were treated by using *disturbance recognition* and *disturbance elimination* based route. The disturbance detection step is the most important part for non-targets disturbance counteraction. The disadvantage of [54] is that the proposed method can only treat very limited kinds of disturbances. However, it is known that there are thousands of "non-target" disturbances in real-world. Therefore, we claim that non-target disturbances counteraction is another huge challenge of E-nose for real applications.
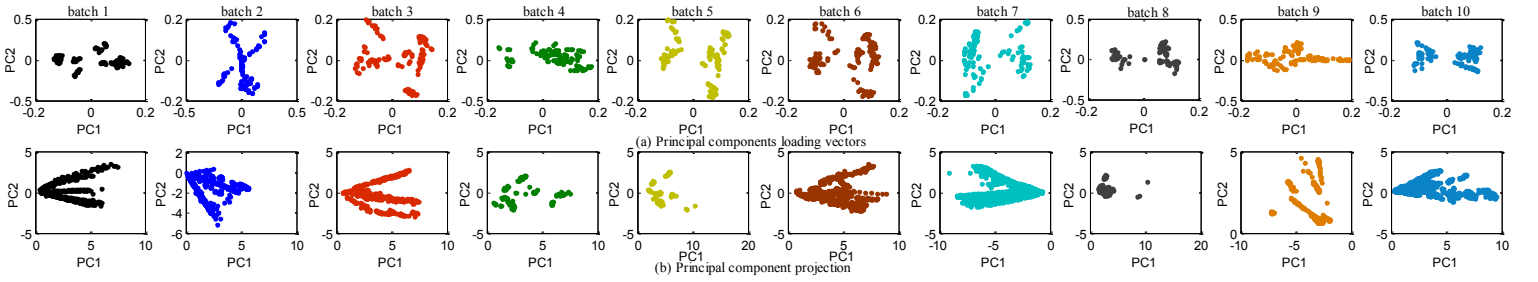
Fig. 6. Principal components loading vectors (a) and principal component projection (b) of the raw data from batch 1 (no drift)
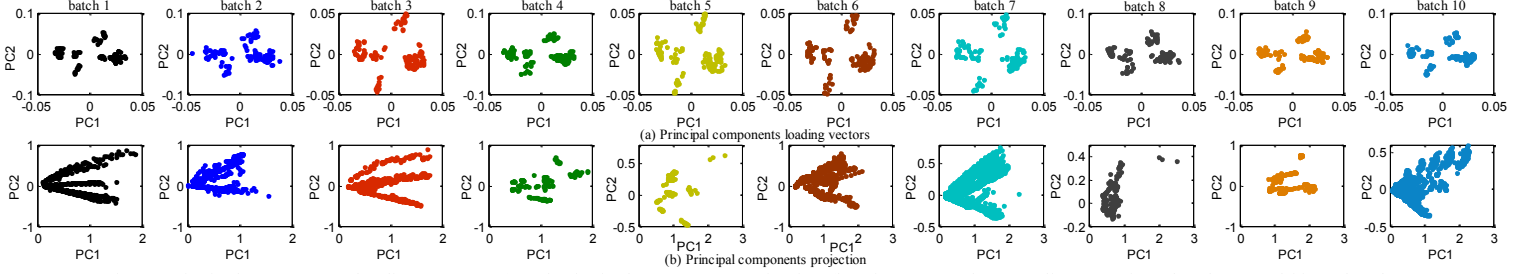
Fig. 7. Principal components loading vectors (a) and principal component projection (b) after UFA subspace alignment from batch 1 (no drift) to batch 10

TABLE I
MEAN DISTRIBUTION DISCREPANCY (MDD) BETWEEN EACH BATCH AND THE BATCH 1 IN LOADING VECTORS AND THE PROJECTION, RESPECTIVELY

MDD	Batch 1	Batch 2	Batch 3	Batch 4	Batch 5	Batch 6	Batch 7	Batch 8	Batch 9	Batch 10	Average
Sample No.	*445*	*1244*	*1586*	*161*	*197*	*2300*	*3613*	*294*	*470*	*3600*	*-*
Loadings_RAW	0	0.0197	0.0185	0.0209	0.0152	0.0194	0.0183	0.0211	0.0160	0.0226	0.0191
Loadings_UFA	0	**0.0065**	**0.0043**	**0.0049**	**0.0075**	**0.0042**	**0.0049**	**0.0059**	**0.0064**	**0.0038**	**0.0054**
Projection_RAW	0	0.0241	0.0186	0.0495	0.0348	0.0222	0.0517	**0.0207**	**0.0725**	0.0257	0.0355
Projection_UFA	0	**0.0220**	**0.0180**	**0.0359**	**0.0328**	**0.0212**	**0.0242**	0.0252	**0.0128**	**0.0260**	**0.0242**

TABLE II
CLASSIFICATION ACCURACY OF OTHER BATCHES USING THE CLASSIFIER LEARNED ON BATCH 1

Accuracy	Batch 1	Batch 2	Batch 3	Batch 4	Batch 5	Batch 6	Batch 7	Batch 8	Batch 9	Batch 10	Average
RAW$_{SVM}$	-	56.1	81.3	63.9	70.1	69.1	47.8	45.6	49.1	31.1	57.1
CCPCA	-	67.0	48.5	41.0	35.5	55.0	31.0	**56.5**	46.5	30.5	45.7
SSL		42.3	73.7	75.5	66.8	**77.5**	**54.4**	33.5	23.6	**34.9**	53.6
UFA$_{SVM}$	-	**74.7**	**83.7**	**79.5**	**75.1**	69.8	47.2	44.2	**66.4**	30.4	**63.4**

● **Targets-to-Targets Self-representation Classifier (T³SRC)**

Hopefully, in this paper, we will propose a novel *Targets-to-Targets Self-representation Classifier* (T³SRC) method and a very effective solution to address this issue. Motivated by dictionary learning based representation classifier theory, the main idea of the proposed T³SRC is that the knowledge of the target gases can be only memorized via knowledge representation learning without depending on what disturbances are damaging the E-nose. That is, the target gases are invariant though the disturbances are ever-changing. The learned model $\boldsymbol{\alpha}$ via T³SRC is recognized as a representation based classifier, which is used for separating the target gases and non-target disturbances by leveraging the representation error as a metric. It is rational to imagine that for some non-target disturbance the representation error would be larger due to the weak representation capability of $\boldsymbol{\alpha}$ on the non-targets. The most prominent merit of the proposed T³SRC is that it can well tackle the fatal flaw in [54] that only very limited disturbances can be treated. Visually, we provide a schematic diagram of T³SRC in Fig.9 for disturbance detection.

Suppose the training set of target gases to be $\mathbf{X} = [\mathbf{x}_1, \cdots, \mathbf{x}_N] \in \mathfrak{R}^{d \times N}$, the self-representation coefficients (i.e. self-classifier) to be $\boldsymbol{\alpha} = [\boldsymbol{\alpha}_1, \cdots, \boldsymbol{\alpha}_N] \in \mathfrak{R}^{N \times N}$, then there is

$$\mathbf{X} = \mathbf{X} \cdot \boldsymbol{\alpha} + \mathbf{E} \qquad (17)$$

where $\mathbf{E}$ denotes the representation error matrix, which implies that some unknown noises may lie in the data. The representation error of $\mathbf{x}_i (i = 1, \cdots, N)$ can be formulated as

$$e_i = \|\mathbf{x}_i - \mathbf{X}\boldsymbol{\alpha}_i\|_2^2, i = 1, \cdots, N \qquad (18)$$

Therefore, a good representation should satisfy that the total representation error (TRE) $\sum_i e_i$ should be minimized, and there is the following model

$$\min_{\boldsymbol{\alpha}} \sum_i e_i = \sum_{i=1}^N \|\mathbf{x}_i - \mathbf{X}\boldsymbol{\alpha}_i\|_2^2 \qquad (19)$$

where $\|\cdot\|_2$ represents l_2-norm. To control the complexity of representation classifier $\boldsymbol{\alpha}$ without overfitting, it is better to use the regularization technique. Therefore, the proposed T³SRC can be compactly formulated by rewritten Eq. (19) with a regularizer as follows

$$\min_{\boldsymbol{\alpha}} \|\mathbf{X} - \mathbf{X}\boldsymbol{\alpha}\|_F^2 + \eta \cdot \mathcal{R}(\boldsymbol{\alpha}) \qquad (20)$$

where $\mathcal{R}(\boldsymbol{\alpha})$ represents some regularizer and η denotes a positive regularization coefficient. In this paper, the L_2-norm regularization based collaborative representation with better robustness and lower computational cost is considered. The
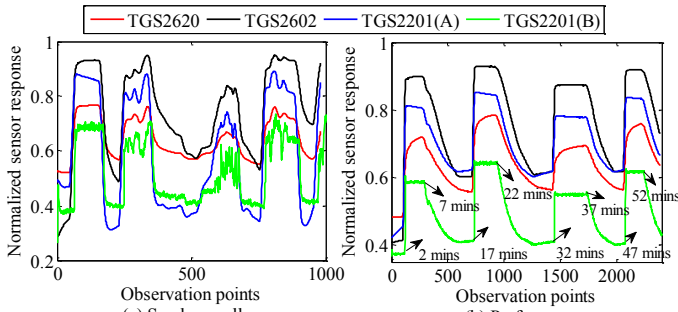
Fig. 8. Sensor response to disturbance, i.e. smoke smell and perfume. (a) and (b) are experimented with different sampling rate.

regularization is a useful way to overcome the noise in classifier learning. Therefore, T^3SRC can be written as

$$\min_{\boldsymbol{\alpha}} \|\mathbf{X} - \mathbf{X}\boldsymbol{\alpha}\|_F^2 + \eta\|\boldsymbol{\alpha}\|_2^2 \qquad (21)$$

It is worth noting that T^3SRC is not used for intra-gases recognition in targets, therefore the label information is unnecessary, which is an unsupervised method for disturbance detection. In this paper, we would like to exploit the representation error boundary idea between *targets-to-targets* and *targets-to-non-targets* for discrimination of targets and non-targets. The closed form solution of Eq. (21) can be achieved as follows

$$\boldsymbol{\alpha} = (\mathbf{X}^T\mathbf{X} + \eta\mathbf{I})^{-1}\mathbf{X}^T\mathbf{X} \qquad (22)$$

In discrimination of targets and non-target, for a new pattern $\mathbf{y} \in \Re^d$, the total representation error (TRE) metric is calculated as

$$TRE_{\mathbf{y}} = \sqrt{\frac{1}{N}\sum_{i=1}^{N}\|\mathbf{y} - \mathbf{X}\boldsymbol{\alpha}_i\|_2^2} \qquad (23)$$

It is clear from Eq. (21) that if one new pattern $\mathbf{y}$ is not from the self-representation set $\mathbf{X}$, then there should be

$$TRE_{\mathbf{y}} > TRE_{\mathbf{x}_i}, \forall i = 1, \cdots, N \qquad (24)$$

It is not difficult to figure out that the representation ability of target by using $\mathbf{X}$ and $\boldsymbol{\alpha}$ is superior to that of non-targets. Then, the attribute decision of $\mathbf{y}$ can be made as follows

$$\text{Attribute}_{\mathbf{y}} = \begin{cases} \text{targets}, & \text{if } TRE_{\mathbf{y}} \leq E_{\text{boundary}} \\ \text{nontargets}, & \text{if } TRE_{\mathbf{y}} > E_{\text{boundary}} \end{cases} \qquad (25)$$

where E_{boundary} represents the boundary of the total representation error, determined by the target testing set and non-target validation set. From the Eq. (21), the solution in Eq. (22) and decision in Eq. (23, 25), we can see that during the process of non-targets discrimination, only the training patterns of the target gases are required. Additionally, the proposed method is an unsupervised manner without using class labels.

● **Experiments**

In this section, we adopt the dataset in [54] for experimental analysis. Six kinds of target gases including formaldehyde (188), benzene (72), toluene (66), carbon monoxide (58), ammonia (60), and nitrogen dioxide (38) are experimented. Note that the digits in brackets denote the number of samples. For learning the T^3SRC model, 10 samples are selected as training set from each gas, respectively and totally 60 samples are used for model training. The remaining data are used for determining the E_{boundary} (test process). In validation process, we have also collected a non-target disturbance (alcohol) data
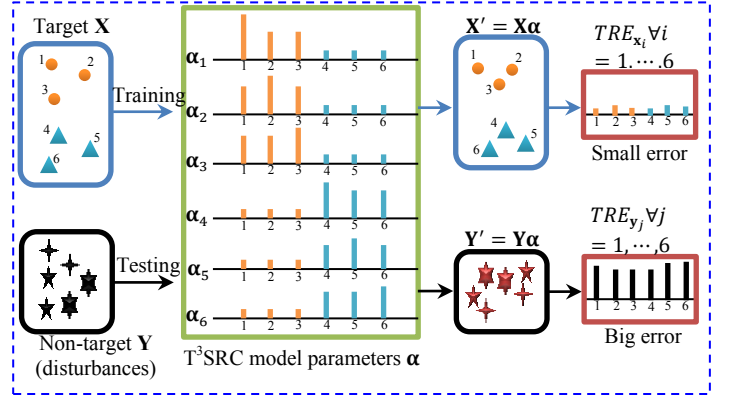
Fig. 9. Schematic diagram of T^3SRC method in training and testing. $\boldsymbol{\alpha}_i$ denotes the representation coefficient vector of the sample $\mathbf{x}_i$ ($i=1,...,6$). The $\alpha_{i,i}$ *w.r.t.* $\mathbf{x}_i$ or of the same class has the largest coefficient, and a small value is obtained *w.r.t.* that of different classes.

Algorithm 2: T^3SRC
Input: Target train-set $\mathbf{X}$, target test-set $\mathbf{Y}$, non-target validation-set $\mathbf{Z}$, and a new pattern $\mathbf{y}$;
Step 1: Calculate $\boldsymbol{\alpha}$ by using Eq. (22);
Step 2: Calculate $TRE_{\mathbf{Y}}$ by using Eq. (23);
Step 3: Calculate $TRE_{\mathbf{Z}}$ by using Eq. (23);
Step 4: Calculate the E_{boundary} by calculating the recognition rate.
Step 5: Calculate $TRE_{\mathbf{y}}$ using Eq. (23) and the Attribute$_{\mathbf{y}}$ using Eq. (25).
Output: $\boldsymbol{\alpha}$, E_{boundary}, Attribute$_{\mathbf{y}}$

set including 48 samples for testing the pre-determined representation error boundary, i.e. E_{boundary}. The total representation error curve of training, testing and validation set is shown in Fig. 10 (a), in which we can see that the non-target disturbance (alcohol) has significantly larger representation error and the target test data has similar errors with the target training data. It also shows the potential capability of the proposed method for differentiating the non-target disturbances by using the representation error based metric. For finding the error boundary for separation by using the representation errors of target testing data, we plot the recognition rate based on Eq. (25) by increasing the error boundary from the lowest error of target testing to the largest error in Fig. 10(b), from which we can observe the $E_{\text{boundary}} = 0.84$ for the best separation between the targets and non-targets. The recognition rates of targets and non-targets are 91.7% and 95.8%, respectively. The ROC (Receiver Operating Characteristic) curve is shown in Fig. 10(c), from which we can clearly observe the good performance of targets and non-targets discrimination. Fig. 10 demonstrates that the targets have very weak representation ability to non-targets. Therefore, it is rational to separate between them by using target-specific representation coefficients with an error boundary (threshold).

Additionally, we have collected another three real-time data with continuous observations, including smoke smell, perfume and mixtures (target vs. non-targets). The average sensor responses have been illustrated in Fig. 11 (first row), from which there are several wave peaks denoting the disturbances. Fig.10 (second row) denotes the total representation error (TRE) of each observation computed as Eq. (23). Notably the *red dashed line* denotes the error (threshold) $E_{boundary}$=0.84 shown

(a) TRE curve

(b) Recognition Rate Curve

(c) Receiver Operating Characteristic Curve
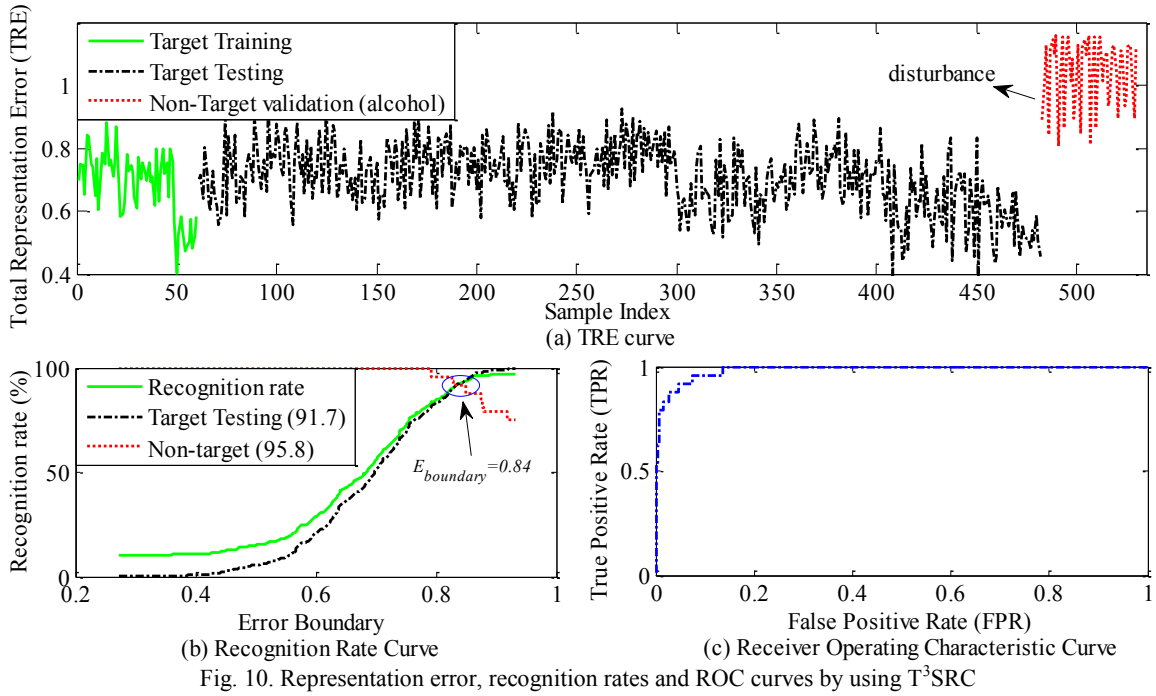
Fig. 10. Representation error, recognition rates and ROC curves by using T³SRC

(a) Nontarget: Smoke smell

(b) Nontarget: Perfume

(c) Mixture of Target and Nontarget
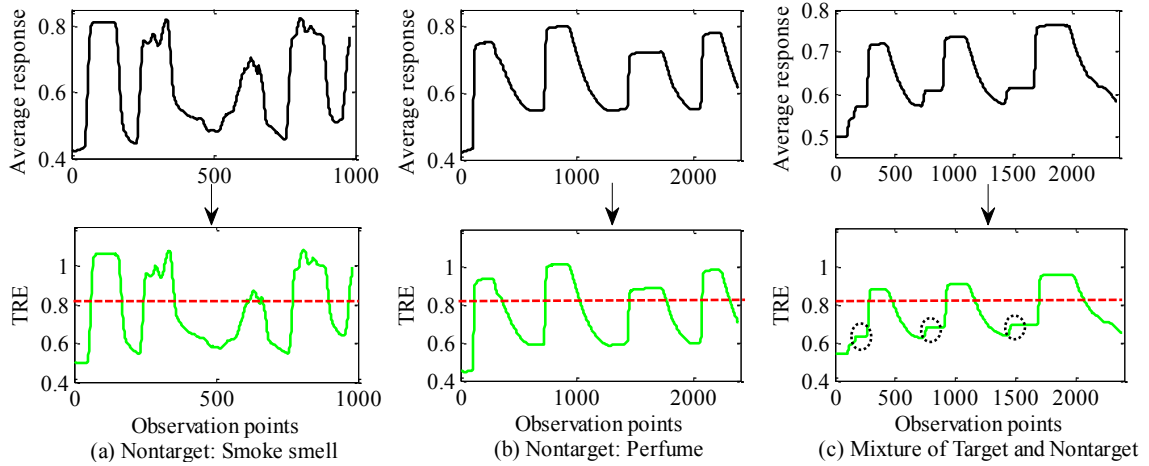
Fig. 11. Representation errors of three continuous observation sets, in which the red dashed line denotes the error boundary for separating between the targets and non-targets (disturbances)

in Fig. 10(b). We can see that the peaks representing disturbance have larger error than $E_{boundary}$ and the attribute recognition is correctly done (100% accuracy). It is worth noting that in Fig. 11(c), the targets are highlighted in ellipses, which have smaller errors than $E_{boundary}$ and the attribute recognition can also be correctly done.

From the experiments, we see that the proposed method is very effective in discrimination of non-targets. The main advantages of T³SRC are threefold: 1) the computation complexity is very low with a closed form solution. 2) in modeling and discrimination, the information of non-targets are not required, which handles the most important and difficult issue in E-noses that thousands of non-target disturbances may exist in real-world. 3) in modeling, very few number of target training samples are used (in this paper, 10 sample for each target gas), such that the computational and manual cost are very low for learning the representation coefficients **α**.

Through analysis of the proposed solutions (GAT, UFA and T³SRC) *w.r.t.* the 3D issues, we provide following remarks:
- The three methods are discussed separately, and used for respective scenarios in a general case.
- More complex conditions that discreteness, drift and disturbance happen simultaneously are not considered.
- For GAT, the calibration coefficients are computed off-line by using several selected data points, and the calibration transfer is on-line with the coefficients.
- For T³SRC, the target gas mixture is not considered, but we assume that the mixture of target gases cannot be non-targets.

IV. CONCLUSION

In this paper, we have summarized the progress and new challenges in E-noses. *First*, the progress is described in application, system and algorithm levels. Specifically, the extensive applications and several different types of E-noses

including conventional E-noses, temperature modulated E-noses, differential E-noses, and active E-noses have been explored. The state-of-the-art algorithms in feature extraction, pattern recognition and drift compensation are overviewed. *Second*, with a deep insight of the observed achievements in E-nose, we present new challenges that have not been properly handled and treated, *i.e.* 3D issues including: (I) Discreteness: sensor reproducibility enhancement; (II) Drift: sensor drift recovery; (III) Disturbance: non-targets disturbances counteraction. *Third*, motivated by these proposed 3D challenges, to this end, we have also proposed the efficient solutions including global affine transformation (GAT), unsupervised feature adaptation (UFA) and targets-to targets self-representation classifier (T^3SRC) for handling the 3D issues to be solved, separately. Experiments demonstrate the effectiveness and efficiency of the proposed approaches in dealing with the proposed issues. Notably, this paper proposes to solve the 3D issues separately with different approaches. A potential limitation of the proposed methods for each issue is the application scenario with gas mixtures, instead of single gas, which would be particularly explored in our future work.

As recent progress in machine learning and feature extraction developed based on different systems [100-104], in the future work, the further improvements can be done in two facets. *First,* in the proposed UFA method, the drift is handled by aligning the principal loading vectors between the clean data and the drifted data. It is also rational to consider the adaptation in some discriminative subspace with better separable capability, such that the drifted data can be reconstructed by the clean data in the subspace. The reconstruction error can be understood to be drift-induced, and the reconstructed new data can be recognized as the drift-less data. The reconstruction process is denoted as drift recovery. *Second,* in the proposed T^3SRC, the L_2-norm is imposed on the representation coefficients $\boldsymbol{\alpha}$ for reducing the complexity caused by overfitting and Gaussian noise. Consider that $\boldsymbol{\alpha}$ has different representation ability to different objects, a stronger sparse constraint on $\boldsymbol{\alpha}$ may be better for discriminative representation. Therefore, L_0 or L_1-norm can be imposed for regularization $\mathcal{R}(\boldsymbol{\alpha})$ in model (20), such that Laplacian noise or outliers can be well fitted.

REFERENCES

[1] K. Persaud and G. Dodd, "Analysis of discrimination mechanisms in the mammalian olfactory system using a model nose," Nature, vol. 299, pp. 352-355, Sep 1982.

[2] J.W. Gardner and P.N. Bartlett, "A Brief History of Electronic Noses," Sensors and Actuators B: Chemical, vol. 18-19, no. 1, pp. 210-211, Mar 1994.

[3] F. Röck, N. Barsan, and U. Weimar, "Electronic Nose: Current Status and Future Trends," Chem. Rev, vol. 108, pp. 705-725, 2008.

[4] K. Brudzewski, S. Osowski, and T. Markiewicz, "Classification of milk by means of an electronic nose and SVM neural network," Sensors and Actuators B: Chemical, vol. 98, pp. 291-298, 2004.

[5] P.C. Lorenzen, H.G. Walte, B. Bosse, "Development of a method for butter type differentiation by electronic nose technology," Sensors and Actuators B: Chemical, vol. 181, pp. 690-693, 2013.

[6] N. Bhattacharyya, R. Bandyopadhyay, M. Bhuyan, B. Tudu, D. Ghosh, and A. Jana, "Electronic Nose for Black Tea Classification and Correlation of Measurement with "Tea Taster" Marks," IEEE Trans Instrumentation and Measurement, vol. 57, no. 7, pp. 1313-1321, Jul 2008.

[7] Q. Chen, J. Zhao, Z. Chen, H. Lin, D.A. Zhao, "Discrimination of green tea quality using the electronic nose technique and the human panel test, comparison of linear and nonlinear classification tools," Sensors and Actuators B: Chemical, vol. 159, no. 1, pp. 294-300, 2011.

[8] R. Dutta, E.L. Hines, J.W. Gardner, K.R. Kashwan, and M. Bhuyan, "Tea quality prediction using a tin oxide-based electronic nose: an artificial intelligent approach," Sensors and Actuators B: Chemical, vol. 94, pp. 228-237, 2003.

[9] G. Hui, Y. Wu, D. Ye, and W. Ding, "Fuji Apple Storage Time Predictive Method Using Electronic Nose," Food Anal. Methods, vol. 6, pp. 82-88, 2013.

[10] M.G. Varnamkhasti, S.S. Mohtasebi, M. Siadat, J. Lozano, H. Ahmadi, S.H. Razavi, A. Dicko, "Aging fingerprint characterization of beer using electronic nose," Sensors and Actuators B: Chemical, vol. 159, no. 1, pp. 51-59, Nov 2011.

[11] M. Peris, L.E. Gilabert, "A 21st century technique for food control: Electronic noses," Analytica Chimica Acta, vol. 638, pp. 1-15, 2009.

[12] A. Berna, "Metal Oxide Sensors for Electronic Noses and Their Application to Food Analysis," Sensors, vol. 10, pp. 3882-3910, 2010.

[13] E.A. Baldwin, J. Bai, A. Plotto, and S. Dea, "Electronic Noses and Tongues: Applications for the Food and Pharmaceutical Industries," Sensors, vol. 11, pp. 4744-4766, 2011.

[14] A. D'Amico, C. Di Natale, R. Paolesse, A. Macagnano, E. Martinelli, G. Pennazza, M. Santonico, M. Bernabei, C. Roscioni, G. Galluccio, "Olfactory systems for medical applications," Sensors and Actuators B: Chemical, vol. 130, pp. 458-465, 2008.

[15] K. Yan and D. Zhang, "Feature selection and analysis on correlated gas sensor data with recursive feature elimination," Sensors and Actuators B: Chemical, vol. 212, pp. 353-363, 2015.

[16] C. Di Natale, A. Macagnano, E. Martinelli, R. Paolesse, G. D'Arcangelo, C. Roscioni, A.F. Agro, A. D'Amico, "Lung cancer identification by the analysis of breath by means of an array of non-selective gas sensosrs," Biosensors and Bioelectronics, vol. 18, pp. 1209-1218, 2003.

[17] A.K. Pavlou, N. Magan, C. McNulty, J.M. Jones, D. Sharp, J. Brown, A.P.F. Turner, "Use of an electronic nose system for diagnoses of urinary tract infections," Biosensors and Bioelectronics, vol. 17, pp. 893-899, 2002.

[18] J. Getino, M.C. Horrillo, J. Gutiérrez, L. Arés, J.I. Robla, C. Garcia, and I. Sayago, "Analysis of VOCs with a tin oxide sensor array," Sensors and Actuators B: Chemical, vol. 43, pp. 200-205, 1997.

[19] E.J. Wolfrum, R.M. Meglen, D. Peterson, J. Sluiter, "Metal oxide sensor arrays for the detection, differentiation, and quantification of volatile organic compounds at sub-part-per-million concentration levels," Sensors and Actuators B: Chemical, vol. 115, pp. 322-329, 2006.

[20] L. Zhang, F. Tian, C. Kadri, G. Pei, H. Li, and L. Pan, "Gases concentration estimation using heuristics and bio-inspired optimization models for experimental chemical electronic nose," Sensors and Actuators B: Chemical, vol. 160, no. 1, pp. 760-770, 2011.

[21] L. Zhang, F. Tian, S. Liu, J. Guo, B. Hu, Q. Ye, L. Dang, X. Peng, C. Kadri, and J. Feng, "Chaos based neural network optimization for concentration estimation of indoor air contaminants by an electronic nose," Sensors and Actuators A: Physical, vol. 189, pp. 161-167, Jan 2013.

[22] L. Dentoni, L. Capelli, S. Sironi, R.D. Rosso, S. Zanetti, and M.D. Torre, "Development of an Electronic Nose for Environmental Odour Monitoring," Sensors, vol. 12, pp. 14363-14381, 2012.

[23] R.E. Baby, M. Cabezas, and E.N.W. de Reca, "Electronic nose: a useful tool for monitoring environmental contamination," Sensors and Actuators B: Chemical, vol. 69, pp. 214-218, 2000.

[24] A. Fort, N. Machetti, S. Rocchi, M.B.S. Santos, L. Tondi, N. Ulivieri, V. Vignoli, and G. Sberveglieri, "Tin Oxide Gas Sensing: Comparison Among Different Measurement Techniques for Gas Mixture Classification," IEEE Trans. Instrumentation and Measurement, vol. 52, no. 3, pp. 921-926, 2003.

[25] J.W. Gardner, H.W. Shin, E.L. Hines, and C.S. Dow, "An electronic nose system for monitoring the quality of potable water," Sensors and Actuators B: Chemical, vol. 69, pp. 336-341, 2000.

[26] M. Cano, V. Borrego, J. Roales, J. Idígoras, T.L. Costa, P. Mendoza, and

J.M. Pedrosa, "Rapid discrimination and counterfeit detection of perfumes by an electronic olfactory system," Sensors and Actuators B: Chemical, vol. 156, pp. 319-324, 2011.

[27] K. Brudzewski, S. Osowski, and A. Golembiecka, "Differential electronic nose and support vector machine for fast recognition of tobacco," Expert Systems with Applications, vol. 39, pp. 9886-9891, 2012.

[28] K. Brudzewski, S. Osowski, and A. Dwulit, "Recognition of Coffee Using Differential Electronic Nose," IEEE Trans. Instrumentation and Measurement, vol. 61, no. 6, pp. 1803-1810, 2012.

[29] P. Ciosek, Z. Brzózka, and W. Wróblewski, "Classification of beverages using a reduced sensor array," Sensors and Actuators B: Chemical, vol. 103, pp. 76-83, 2004.

[30] K. Brudzewski, S. Osowski, and W. Pawlowski, "Metal oxide sensor arrays for detection of explosives at sub-parts-per million concentration levels by the differential electronic nose," Sensors and Actuators B: Chemical, vol. 161, pp. 528-533, 2012.

[31] A.D. Wilson and M. Baietto, "Applications and Advances in Electronic-Nose Technologies," Sensors, vol. 9, pp. 5099-5148, 2009.

[32] L. Zhang and F. Tian, "Performance Study of Multilayer Perceptrons in a Low-Cost Electronic Nose," IEEE Trans. Instrumentation and Measurement, vol. 63, no. 7, pp. 1670-1679, Jul 2014.

[33] L. Zhang, F. Tian, X. Peng, X. Yin, G. Li and L. Dang, "Concentration estimation using metal oxide semi-conductor gas sensor array based e-noses," Sensor Review, vol. 34, pp. 284-290, 2014.

[34] H.K. Hong, C.H. Kwon, S.R. Kim, D.H. Yun, K. Lee, and Y.K. Sung, "Portable electronic nose system with gas sensor array and artificial neural network," Sensors and Actuators B: Chemical, vol. 66, pp. 49-52, 2000.

[35] I.R. Lujan, J. Fonollosa, A. Vergara, M. Homer, and R. Huerta, "On the calibration of sensor arrays for pattern recognition using the minimal number of experiments," Chemometrics and Intelligent Laboratory Systems, vol. 130, pp. 123-134, 2014.

[36] A.P. Lee and B.J. Reedy, "Temperature modulation in semiconductor gas sensing," Sensors and Actuators B: Chemical, vol. 60, pp. 35-42, 1999.

[37] E. Llobet, R. Ionescu, S.A. Khalifa, J. Brezmes, X. Vilanova, X. Correig, N. Barsan and J.W. Gardner, "Multicomponent Gas Mixture Analysis Using a Single Tin Oxide Sensor and Dynamic Pattern Recognition," IEEE Sensors Journal, vol. 1, no. 3, pp. 207-213, Oct 2001.

[38] E. Martinelli, D. Polese, A. Catini, A. D'Amico, and C. Di Natale, "Self-adapted temperature modulation in metal-oxide semiconductor gas sensors," Sensors and Actuators B: Chemical, vol. 161, pp. 534-541, 2012.

[39] F. Hossein-Babaei and A. Amini, "A breakthrough in gas diagnosis with a temperature-modulated generic metal oxide gas sensor," Sensors and Actuators B: Chemical, vol. 166-167, pp. 419-425, 2012.

[40] F. Hossein-Babaei and A. Amini, "Recognition of complex odors with a single generic tin oxide gas sensor," Sensors and Actuators B: Chemical, vol. 194, pp. 156-163, 2014.

[41] X. Yin, L. Zhang, F. Tian, and D. Zhang, "Temperature Modulated Gas Sensing E-nose System for Low-cost and Fast Detection," IEEE Sensors Journal, 2015. Doi: 10.1109/JSEN.2015.2483901

[42] R. Gosangi and R. Gutierrez-Osuna, "Active Temperature Programming for Metal-Oxide Chemoresistors," IEEE Sensors Journal, vol. 10, no. 6, pp. 1075-1082, Jun 2010.

[43] R. Gosangi and R. Gutierrez-Osuna, "Active temperature modulation of metal-oxide sensors for quantitative analysis of gas mixtures," Sensors and Actuators B: Chemical, vol. 185, pp. 201-210, 2013.

[44] F. Herrero-Carrón, D.J. Yáñez, F.D.B. Rodríguez, and P. Varona, "An active, inverse temperature modulation strategy for single sensor odorant classification," Sensors and Actuators B: Chemical, vol. 206, pp. 555-563, 2015.

[45] M. Imahashi and K. Hayashi, "Odor clustering and discrimination using an odor separating system," Sensors and Actuators B: Chemical, vol. 166-167, pp. 685-694, 2012.

[46] S.K. Jha and K. Hayashi, "A novel odor filtering and sensing system combined with regression analysis for chemical vapor quantification," Sensors and Actuators B: Chemical, vol. 200, pp. 269-287, 2014.

[47] S.M. Scott, D. James, and Z. Ali, "Data analysis for electronic nose systems," Microchim Acta, vol. 156, pp. 183-207, 2007.

[48] X. Peng, L. Zhang, F. Tian, and D. Zhang, "A novel sensor feature extraction based on kernel entropy component analysis for discrimination of indoor air contaminants," Sensors and Actuators A: Physical, vol. 234, pp. 143-149, 2015.

[49] E. Martinelli, C. Falconi, A. D'Amico, and C. Di Natale, "Feature Extraction of chemical sensors in phase space," Sensors and Actuators B: Chemical, vol. 95, pp. 132-139, 2003.

[50] A. Leone, C. Distante, N. Ancona, K.C. Persaud, E. Stella, and P. Siciliano, "A powerful method for feature extraction and compression of electronic nose responses," Sensors and Actuators B: Chemical, vol. 105, pp. 378-392, 2005.

[51] L. Zhang, F. Tian, and G. Pei, "A novel sensor selection using pattern recognition technique in electronic nose," Measurement, vol. 54, pp. 31-39, 2014.

[52] B. Ehret, K. Safenreiter, F. Lorenz, and J. Biermann, "A new feature extraction method for odour classification," Sensors and Actuators B: Chemical, vol. 158, pp. 75-88, 2011.

[53] R. Kaur, R. Kumar, A. Gulati, C. Ghanshyam, P. Kapur, A.P. Bhondekar, "Enhancing electronic nose performance: A novel feature selection approach using dynamic social impact theory and moving window time slicing for classification of Kangra orthodox black tea (*Camellia sinensis* (L.) O. Kuntze)," Sens. Actuators B: Chem, vol. 166-167, pp. 309-319, 2012.

[54] L. Zhang, F. Tian, L. Dang, G. Li, X. Peng, X. Yin, and S. Liu, "A novel background interferences elimination method in electronic nose using pattern recognition," Sensors and Actuators A: Physical, vol. 201, pp. 254-263, Oct 2013.

[55] L. Zhang, F. Tian, S. Liu, H. Li, C. Kadri, and L. Pan, "Applications of Adaptive Kalman Filter Coupled with Multilayer Perceptron for Quantification Purposes in Electronic Nose," Journal of Computational Information Systems, vol. 8, pp. 275-282, 2012.

[56] S.K. Jha and R.D.S. Yadava, "Denosing by Singular Value Decomposition and Its Application to Electronic Nose Data Processing," IEEE Sensors Journal, vol. 11, no. 1, pp. 35-44, Jan 2011.

[57] A. Van der Veen, E.F. Deprettere, and A.L. Swindlehurst, "Subspace based signal analysis using singular value decomposition," Proceedings of the IEEE, vol. 81, no. 9, pp. 1277-1308, Sep 1993.

[58] C. Di Natale, E. Martinelli, and A. D'Amico, "Counteraction of environmental disturbances of electronic nose data by independent component analysis," Sensors and Actuators B: Chemical, vol. 82, pp. 158-165, 2002.

[59] M. Kermit and O. Tomic, "Independent Component Analysis Applied on Gas Sensor Array Measurement Data," IEEE Sensors Journal, vol. 3, no. 2, pp. 218-228, 2003.

[60] F. Tian, H. Li, L. Zhang, S. Liu, Q. Ye, B. Hu, and B. Xiao, "A Denoising Method based on PCA and ICA in Electronic Nose for Gases Quantification," Journal of Computational Information Systems, vol. 8, pp. 5005-5015, 2012.

[61] A. Hyvärinen and E. Oja, "Independent component analysis: Algorithms and applications," Neural Networks, vol. 13, no. 4-5, pp. 411-430, 2000.

[62] S. Marco and A.G. Gálvez, "Signal and Data Processing for Machine Olfaction and Chemical Sensing: A Review," IEEE Sensors Journal, vol. 12, no. 11, Nov 2012.

[63] S. Güney and A. Atasoy, "Multiclass classification of n-butanol concentrations with k-nearest neighbor algorithm and support vector machine in an electronic nose," Sensors and Actuators B: Chemical, vol. 166-167, pp. 721-725, 2012.

[64] K.T. Tang, Y.S. Lin, and J.M. Shyu, "A local weighted nearest neighbor algorithm and a weighted and constrained least-squared method for mixed odor analysis by electronic nose systems," Sensors, vol. 10, pp. 10467-10483, 2010.

[65] S. Omatu and M. Yano, "E-nose system by using neural networks," Neurocomputing, vol. 172, pp. 394-398, 2016.

[66] Z. Xu, X. Shi, L. Wang, J. Luo, C.J. Zhong, and S. Lu, "Pattern recognition for sensor array signals using Fuzzy ARTMAP," Sensors and Actuators B: Chemical, vol. 141, pp. 458-464, 2009.

[67] D. Gao, Z. Yang, C. Cai, and F. Liu, "Performance evaluation of multilayer perceptrons for discriminating and quantifying multiple kinds of odors with an electronic nose," Neural Networks, vol. 33, pp. 204-215, 2012.

[68] D. Gao, F. Liu, and J. Wang, "Quantitative analysis of multiple kinds of volatile organic compounds using hierarchical models with an electronic nose," Sensors and Actuators B: Chemical, vol. 161, pp. 578-586, 2012.

[69] S.J. Dixon and R.G. Brereton, "Comparison of performance of five common classifiers represented as boundary methods: Euclidean Distance to Centroids, Linear Discriminant Analysis, Quadratic Discriminant Analysis, Learning Vector Quantization and Support Vector Machines, as dependent on data structure," Chemometrics and Intelligent Laboratory Systems, vol. 95, pp. 1-17, 2009.

[70] J.H. Cho and P.U. Kurup, "Decision tree approach for classification and

dimensionality reduction of electronic nose data," Sensors and Actuators B: Chemical, vol. 160, no. 1, pp. 542-548, 2011.

[71] X. Wang, M. Ye, and C.J. Duanmu, "Classification of data from electronic nose using relevance vector machines," Sensors and Actuators B: Chemical, vol. 140, pp. 143-148, 2009.

[72] L. Zhang, F. Tian, H. Nie, L. Dang, G. Li, Q. Ye, and C. Kadri, "Classification of multiple indoor air contaminants by an electronic nose and a hybrid support vector machine," Sensors and Actuators B: Chemical, vol. 174, pp. 114-125, 2012.

[73] A. Vergara, J. Fonollosa, J. Mahiques, M. Trincavelli, N. Rulkov, and R. Huerta, "On the performance of gas sensor arrays in open sampling systems using Inhibitory Support Vector Machines," Sensors and Actuators B: Chemical, vol. 85, pp. 462-477, 2013.

[74] M. Shi, A. Bermak, S.B. Belhouari, and P.C.H. Chan, "Gas Identification Based on Committee Machine for Microelectronic Gas Sensor," IEEE Trans. Instrumentation and Measurement, vol. 55, no. 5, pp. 1786-1793, Oct 2006.

[75] A. Szczurek, B. Krawczyk, and M. Maciejewska, "VOCs classification based on the committee of classifiers coupled with single sensor signals," Chemometrics and Intelligent Laboratory Systems, vol. 125, pp. 1-10, June 2013.

[76] L. Dang, F. Tian, L. Zhang, C. Kadri, X. Yin, X. Peng, and S. Liu, "A novel classifier ensemble for recognition of multiple indoor air contaminants by an electronic nose," Sensors and Actuators A: Physical, vol. 207, pp. 67-74, Mar 2014.

[77] B. Tudu, A. Metla, B. Das, N. Bhattacharyya, A. Jana, D. Ghosh, and R. Bandyopadhyay, "Towards Versatile Electronic Nose Pattern Classifier for Black Tea Quality Evaluation: An Incremental Fuzzy Approach," IEEE Trans. Instrumentation and Measurement, vol. 58, no. 9, pp. 3069-3078, 2009.

[78] S.K. Jha, K. Hayashi, and R.D.S. Yadava, "Neural, fuzzy and neuro-fuzzy approach for concentration estimation of volatile organic compounds by surface acoustic wave sensor array," Measurement, vol. 55, pp. 186-195, 2014.

[79] S. De Vito, G. Fattoruso, M. Pardo, F. Tortorella, and G. Di Francia, "Semi-Supervised Learning Techniques in Artificial Olfaction: A Novel Approach to Classification Problems and Drift Counteraction," IEEE Sensors Journal, vol. 12, no. 11, pp. 3215-3224, 2012.

[80] X. Hong, J. Wang, and G. Qi, "Comparison of semi-supervised and supervised approaches for classification of e-nose datasets: Case studies of tomato juices," Chemometrics and Intelligent Laboratory Systems, vol. 146, pp. 457-463, Aug 2015.

[81] R. Gutierrez-Osuna, "Pattern Analysis for Machine Olfaction: A Review," IEEE Sensors Journal, vol. 2, no. 3, pp. 189-202, June 2002.

[82] M. Holmberg, F.A.M. Davide, C.D. Natale, A. D'Amico, F. Winquist, and I. Lundström, "Drift counteraction in odour recognition applications: Lifelong calibration method," Sensors and Actuators B: Chemical, vol. 42, no. 3, pp. 185-194, Aug 1997.

[83] M. Zuppa, C. Distante, P. Siciliano, and K.C. Persaud, "Drift counteraction with multiple self-organising maps for an electronic nose," Sensors and Actuators B: Chemical, vol. 98, pp. 305-317, 2004.

[84] H. Ding, J.H. Liu, and Z.R. Shen, "Drift reduction of gas sensor by wavelet and principal component analysis," Sensors and Actuators B: Chemical, vol. 96, pp. 354-363, 2003.

[85] T. Artursson, T. Eklov, I. Lundstrom, P. Martensson, M. Sjostrom, and M. Holmberg, "Drift correction for gas sensors using multivariate methods," J. Chemometrics, vol. 14, no. 5-6, pp. 711-723, Dec 2000.

[86] A. Ziyatdinov, S. Marco, A. Chaudry, K. Persaud, P. Caminal, and A. Perera, "Drift compensation of gas sensor array data by common principal component analysis," Sensors and Actuators B: Chemical, vol. 146, pp. 460-465, 2010.

[87] M. Padilla, A. Perera, I. Montoliu, A. Chaudry, K. Persaud, and S. Marco, "Drift compensation of gas sensor array data by Orthogonal Signal Correction," Chemometrics and Intelligent Laboratory Systems, vol. 100, pp. 28-35, 2010.

[88] S. Di Carlo, M. Falasconi, E. Sanchez, A. Scionti, G. Squillero, and A. Tonda, "Increasing pattern recognition accuracy for chemical sensing by evolutionary based drift compensation," Pattern Recognition Letters, vol. 32, pp. 1594-1603, 2011.

[89] L. Zhang, F. Tian, S. Liu, L. Dang, X. Peng, and X. Yin, "Chaotic time series prediction of e-nose sensor drift in embedded phase space," Sensors and Actuators B: Chemical, vol. 182, pp. 71-79, 2013.

[90] A. Vergara, S. Vembu, T. Ayhan, M.A. Ryan, M.L. Homer, and R. Huerta, "Chemical gas sensor drift compensation using classifier ensembles," Sensors and Actuators B: Chemical, vol. 166-167, pp. 320-329, 2012.

[91] H. Liu and Z. Tang, "Metal Oxide Gas Sensor Drift Compensation Using a Dynamic Classifier Ensemble Based on Fitting," Sensors, vol. 13, pp. 9160-9173, 2013.

[92] E. Martinelli, G. Magna, S. DeVito, R. Di Fuccio, G. Di Francia, A. Vergara, and C. Di Natale, "An adaptive classification model based on the Artificial Immune System for chemical sensor drift mitigation," Sensors and Actuators B: Chemical, vol. 177, pp. 1017-1026, 2013.

[93] Q. Liu, X. Li, M. Ye, S.S. Ge, and X. Du, "Drift Compensation for Electronic Nose by Semi-Supervised Domain Adaptation," IEEE Sensors Journal, vol. 14, no. 3, pp. 657

[94] L. Zhang and D. Zhang, "Domain Adaptation Extreme Learning Machines for Drift Compensation in E-nose Systems," IEEE Trans. Instrumentation and Measurement, vol. 64, no. 7, pp. 1790-1801, 2015.

[95] E.J. Wolfrum, R.M. Meglen, D. Peterson, and J. Sluiter, "Calibration transfer among sensor arrays designed for monitoring volatile organic compounds in indoor air quality," IEEE Sensors Journal, vol. 6, no. 6, pp. 1638-1643, Dec 2006.

[96] L. Zhang, F.C. Tian, X.W. Peng, and X. Yin, "A rapid discreteness correction scheme for reproducibility enhancement among a batch of MOS gas sensors," Sensors and Actuators A: Physical, vol. 205, pp. 170-176, 2014.

[97] O. Tomic, H. Ulmer, and J.E. Haugen, "Standardization methods for handling instrument related signal shift in gas-sensor array measurement data," Analytica Chimica Acta, vol. 472, pp. 99-111, 2002.

[98] L. Zhang, F. Tian, X. Peng, L. Dang, G. Li, S. Liu, and C. Kadri, "Standardization of metal oxide sensor array using artificial neural networks through experimental design," Sensors and Actuators B: Chemical, vol. 177, pp. 947-955, 2013.

[99] L. Zhang, F. Tian, C. Kadri, B. Xiao, H. Li, L. Pan, and H. Zhou, "On-line sensor calibration transfer among electronic nose instruments for monitoring volatile organic chemicals in indoor air quality," Sensors and Actuators B: Chemical, vol. 160, pp. 899-909, 2011.

[100] H. Kaindl, M. Vallee, and E. Arnautovic, "Self-Representation for Self-Configuration and Monitoring in Agent-Based Flexible Automation Systems," IEEE Trans. Systems, Man, and Cybernetics: Systems, vol. 43, no. 1, pp. 164-175, 2013.

[101] B. Zhang, W. Li, P. Qing, and D. Zhang, "Palm-Print Classification by Global Features," IEEE Trans. Systems, Man, and Cybernetics: Systems, vol. 43, no. 2, pp. 370-378, 2013.

[102] A.D. Kenyon, V.M. Catterson, S.D.J. McArthur, and J. Twiddle, "An Agent-Based Implementation of Hidden Markov Models for Gas Turbine Condition Monitoring," IEEE Trans. Systems, Man, and Cybernetics: Systems, vol. 44, no. 2, pp. 186-195, 2014.

[103] W. Sheng, S. Chen, G. Xiao, J. Mao, and Y. Zheng, "A Biometric Key Generation Method Based on Semisupervised Data Clustering," IEEE Trans. Systems, Man, and Cybernetics: Systems, vol. 45, no. 9, pp. 1205-1217, 2015.

[104] C. Xiao and W.A. Chaovalitwongse, "Optimization Models for Feature Selection of Decomposed Nearest Nighbor," IEEE Trans. Systems, Man, and Cybernetics: Systems, vol. 46, no. 2, pp. 177-184, 2016.

[105] V. Riffo and D. Mery, "Automated Detection of Threat Objects Using Adapted Implicit Shape Model," IEEE Trans. Systems, Man, and Cybernetics: Systems, vol. 46, no. 4, pp. 472-482, 2016.